


## EDGE ARTICLE

[View Article Online](#)  
[View Journal](#) | [View Issue](#)Cite this: *Chem. Sci.*, 2022, 13, 14300 All publication charges for this article have been paid for by the Royal Society of ChemistryReceived 13th July 2022  
Accepted 9th November 2022

DOI: 10.1039/d2sc03909e

[rsc.li/chemical-science](https://rsc.li/chemical-science)

## Selection of diverse polymorphic structures from a small dynamic molecular network controlled by the environment†

Boris Bartolec, Armin Kiani, Meagan A. Beatty, Meniz Altay, Guillermo Monreal Santiago and Sijbren Otto \*

The complex interplay between systems and their environment plays an important role in processes ranging from self-assembly to evolution. Polymorphism, where, from the same ingredients different products can be formed, is likely to be an important enabler for evolutionary adaptation. Environmental pressures may induce polymorphic behaviour, where different pressures result in different structural organisation. Here we show that by combining covalent and non-covalent bond formation three distinct polymorphs can emerge from the same small dynamic molecular network: vesicular aggregates, self-replicating fibres and nanoribbons, depending on the nature of the solvent environment. Additionally, a particular set of conditions allows the transient co-existence of both vesicles and fibres.

## Introduction

Considering the various chemical conditions that prevailed on Earth at the time life originated, the potential role of environmental parameters in both the origin and evolution of life is significant, but also poorly understood.<sup>1</sup> Under sudden environmental changes, populations adapt to new conditions or risk extinction.<sup>2</sup> This adaption can occur by means of various processes including that of polymorphism.<sup>3–4</sup>

In biology, polymorphism refers to the emergence of multiple specific morphologies from a discrete species as a result of altering the environment.<sup>3</sup> Even within a single cell, many biomacromolecules such as proteins,<sup>4</sup> carbohydrates<sup>5</sup> and lipids<sup>6</sup> are able to assemble into different types of supramolecular polymorphs, while maintaining the chemical structures of the assembling molecules.<sup>7</sup> This phenomenon suggests a subtle interplay of different self-assembly pathways that can be influenced by changes in non-covalent interactions between molecules. For example, changing pH or ionic strength can lead to different forms in tubular polymers of the tobacco mosaic virus capsid protein.<sup>8</sup>

Recently, a number of pioneering studies have shown polymorphism in supramolecular structures.<sup>9</sup> Numerous examples have been reported of single building blocks systems that form diverse polymorphs by changes in the environment such as co-solvent, temperature and concentration.<sup>10</sup> For example, Meijer and co-workers reported a family of carboxylic acid

functionalized water-soluble benzene-1,3,5-tricarboxamides (BTAs) that self-assemble in water into either fibres, membranes, or hollow nanotubes depending on slight changes in the temperature.<sup>11</sup> In another study, the same group reported three different polymorphs from a tetraamide-substituted biphenyl derivative that emerge from different concentrations of water.<sup>12</sup>

Whereas the role of the environment on supramolecular polymorphism has been widely studied, the effects of the environment on the emergence of various polymorphs combined with molecular structure transformation remains relatively rare. Allowing for the interplay between molecular structure and self-assembly adds a level of plasticity that should enhance the access to diverse polymorphs. It is perhaps not surprising that many key processes in biology rely on such interplay (e.g. enzyme catalysis, nucleic acid replication).

Dynamic combinatorial chemistry<sup>13</sup> is a powerful tool for exploring the role of the environment in the emergence of polymorphs and structural adaption as it allows to amalgamate covalent and non-covalent interactions in a way that allows both processes to influence each other. Dynamic combinatorial libraries (DCLs) are formed from building blocks that react with one another forming reversible covalent bonds. The library members interconvert through exchange of building blocks and the library composition can be influenced by the addition of a template or through stabilization of inter/intramolecular interactions between library members. There are many examples of vesicles, micelles and self-replicating fibrous structures that have emerged from DCLs.<sup>14</sup>

We now show that DCLs made from a single building block in aqueous solution give rise to the spontaneous emergence of various morphologies such as vesicular compartments, self-

Centre for Systems Chemistry, Stratingh Institute, University of Groningen, Nijenborgh 4, 9747 AG Groningen, The Netherlands. E-mail: [s.otto@rug.nl](mailto:s.otto@rug.nl)

† Electronic supplementary information (ESI) available. See DOI: <https://doi.org/10.1039/d2sc03909e>



replicator fibres or both simultaneously. Which type of structures form is critically dependent on the environment and controlled by the nature of the organic co-solvent.

## Results and discussion

We previously reported the formation of diverse membranous supramolecular structures in DCLs made from the amphiphilic building block **1**.<sup>15</sup> Upon air oxidation of **1** the dithiol motifs react with one another to form a library of macrocycles of various sizes linked by disulfide bonds. Upon changing the temperature and agitation, vesicles, nanosheets and sponge-like structures emerged. The fact that this system is sensitive to small perturbations prompted us to explore different environmental conditions by modifying the solvent composition. Co-solvents are well established as agents that break hydrophobic interactions<sup>16</sup> and/or swell and fluidise the membrane core of vesicles.<sup>17</sup> These effects rely heavily on the intercalation capabilities of solvent molecules within the assemblies. We envisaged that, using solvent mixtures to prepare DCLs, we would be able to further expand the range of morphologies of the self-assembled structures that can be accessed.

We now show that simple alcohols and polar aprotic solvents offer a simple way to change the composition of DCLs made from building block **1** from membranous structures to fibres, nanoribbons, and vesicular aggregates and from a collection of large macrocycles to the selective formation of smaller oligomers (Scheme 1).

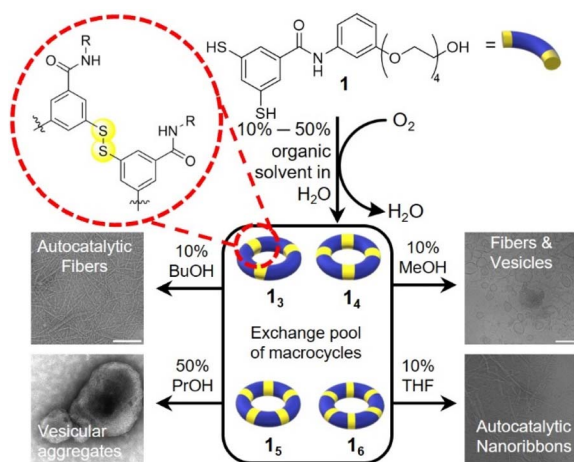
We first explored the DCL made from building block **1** in the presence of 1-propanol. Building block **1** (1.0 mM) was allowed to oxidise in the presence of 10% 1-propanol in B<sub>2</sub>O<sub>3</sub> buffer and the library was monitored by UPLC over 45 days. Macrocycles **1**<sub>5</sub> and **1**<sub>6</sub> emerged together as the two dominant species in the library. Interestingly, different replicate samples yielded different ratios of **1**<sub>4</sub>/**1**<sub>5</sub>/**1**<sub>6</sub>, indicative of stochastic behaviour,

similar to that observed previously with another building block.<sup>18</sup> For instance, in the example in Fig. 1a, **1**<sub>6</sub> completely dominates the library while in another sample, shown in Fig. 1b, **1**<sub>5</sub> transiently formed and then gave way to **1**<sub>4</sub> and other products. However, in most other samples either **1**<sub>6</sub> or **1**<sub>5</sub> were the dominant species (Fig. S1†). These results contrast with the library without co-solvent that forms a wide range of supramolecular structures within one library composed mainly of **1**<sub>4</sub> and other large macrocycles.<sup>15</sup>

Analysis by TEM of samples dominated by **1**<sub>6</sub> or **1**<sub>5</sub> revealed fibres in both cases (Fig. 1c and d). By analogy with the previously observed stochastic systems,<sup>18</sup> these results suggest that under these environmental conditions the system is close to the phase boundary between the different assemblies. At higher 1-propanol content (15%) stochastic behaviour was not observed and several repeats all gave **1**<sub>4</sub> as the dominant macrocycle (Fig. S2†). Table S1† gives an overview of the results obtained in these and other solvent compositions.

The observation that fibre formation in the presence of cosolvent requires a minimum ring size is in line with previous observations on peptide-based analogues of **1**, where the strength of the interactions between the individual building blocks dictates the minimal ring size for fibre formation.<sup>19</sup>

The structure of these fibres resembles that of previously reported peptide-based systems which were found to catalyse their own formation, which classifies them as self-replicators.<sup>14</sup> In order to determine if our current ethylene oxide fibres behaved similarly, seeding experiments were conducted. The addition of pre-formed **1**<sub>6</sub> fibre seed to a solution made from building block **1** (80% oxidized) revealed a faster growth of **1**<sub>6</sub> compared to its growth without seed, indicative of self-replication (Fig. S3†). A similar result was observed upon seeding with pre-formed **1**<sub>5</sub> (Fig. S4†). These results indicate



**Scheme 1** Polymorphs emerging from a single building block dynamic combinatorial library (DCL). Building block **1** is oxidised by air to form a DCL of macrocycles that form various polymorphic structures depending on the co-solvent present. Scale bars = 200 nm.

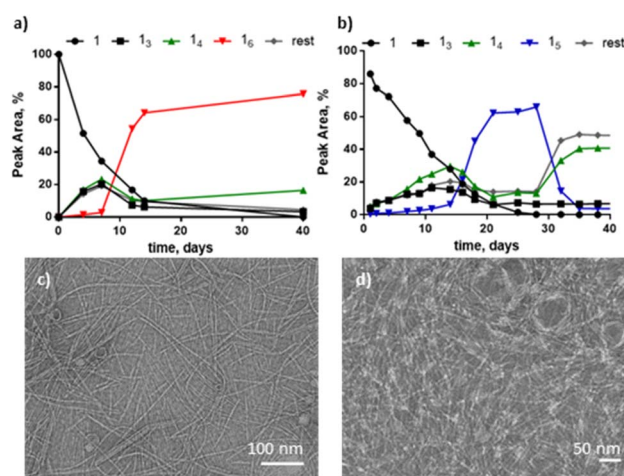


**Fig. 1** Upon air oxidation of dithiol **1** (1.0 mM) in the presence of 10% 1-propanol in B<sub>2</sub>O<sub>3</sub> buffer (50 mM, pH 8.0), **1**<sub>5</sub> and **1**<sub>6</sub> macrocycles emerge and yield fibrous structures. The plasticity of the system is exemplified by two representative replicates yielding two different outcomes: (a) one replicate forms **1**<sub>6</sub> as the main species while (b) the second replicate yields **1**<sub>5</sub>, yet TEM analysis (negative staining) of both samples, (c) and (d), respectively, show fibres as the main polymorph.



that **1<sub>6</sub>** and **1<sub>5</sub>** are self-replicators in this specific solvent environment.

Upon increasing the concentration of 1-propanol (to 50%) fibres no longer formed, but instead vesicular aggregates were obtained. After 1 month a sample made from building block **1** in the presence of 50% 1-propanol in B<sub>2</sub>O<sub>3</sub> buffer yielded **1<sub>4</sub>** as the dominant species (similarly to samples without co-solvent) (Fig. 2a). TEM micrographs revealed large vesicular aggregates with distinct periodic deformities and an average size of 50–100 nm (Fig. 2b and S5†). These unusual structures are very similar to the negatively stained multilamellar liposomes previously reported.<sup>20</sup> Interested in the possible self-reproduction of these vesicle-like structures, we conducted similar seeding experiments as before. Pre-formed **1<sub>4</sub>** solution was added to a sample made from **1**, however, no autocatalysis in the formation of **1<sub>4</sub>** was observed (Fig. S6†). We speculate that 1-propanol is likely to insert into the assemblies, increasing their hydrophobic volume. In analogy with the packing parameter<sup>21</sup> analysis in surfactant chemistry, where increasing the hydrophobic volume of a surfactant causes a transition from (worm-like) micellar to bilayer aggregates, we suspect that such increase in hydrophobic volume might cause a transition from fibrous assemblies to vesicles. This transition is accompanied by a reduction in ring size to yield tetramers, which might pack better in the vesicular aggregates.

Using 1-butanol as a co-solvent at low concentrations yielded results that were similar to those obtained with 1-propanol at similar concentrations. Building block **1** (1.0 mM) was stirred (1200 rpm) at room temperature in the presence of 10% 1-butanol in B<sub>2</sub>O<sub>3</sub> buffer (50 mM, pH 8.5) and the sample was monitored by UPLC over the course of 40 days. Initially, **1<sub>5</sub>** dominated the library but after two weeks **1<sub>5</sub>** partially gave way to **1<sub>6</sub>**. After 40 days, both macrocycles co-existed (Fig. S7a†) and TEM micrographs revealed the formation of fibrous structures (Fig. S7b†).

Also when using ethanol as the co-solvent the same macrocycles emerged, albeit more slowly. After 4 months, in a sample made from building block **1** in the presence of 10% ethanol, **1<sub>5</sub>** and **1<sub>6</sub>** dominated the library together and TEM micrographs again revealed fibre-like structures (Fig. S8†).

The presence of THF induces a novel nanoribbon structure not yet observed for this system. Building block **1** (1.0 mM) was stirred at room temperature in the presence of 10% THF in B<sub>2</sub>O<sub>3</sub> buffer (50 mM, pH 8) and after 40 days **1<sub>6</sub>** was the major species

(Fig. 3a). However, unlike for the alcohols tested before, the TEM micrographs of the THF-containing sample revealed twisted nanoribbons (Fig. 3b). The formation of hexamer nanoribbons occurred in a relatively narrow window of solvent composition as DCLs at 30 and 50% THF were dominated by **1<sub>4</sub>** (Table S1, Fig. S9†). To determine if the ring size or the morphology could be modified by mechanical agitation, two more samples were prepared with 10% THF that were either shaken (1200 rpm) or left non-agitated for 40 days. The shaken sample was dominated by **1<sub>6</sub>** (Fig. S10a†) and resembled the stirred sample while the non-agitated sample contained mainly **1<sub>3</sub>**, **1<sub>4</sub>** along with other larger macrocycles (*e.g.* **1<sub>5</sub>**–**1<sub>7</sub>**) and remained clear (Fig. S10b†). In contrast to the agitated samples, visual inspection of the non-agitated samples gave no indication for large-scale assembly (although we cannot exclude the presence of small aggregates). Seeding a fresh solution made from **1** with pre-formed nanoribbons from the shaken sample significantly accelerated the growth of **1<sub>6</sub>**, in comparison to the non-seeded sample (Fig. 3c), showing that also the nanoribbons form autocatalytically. Thus the hierarchical assembly of fibres into ribbons does not hamper autocatalysis, as was previously reported for the formation of tubular superstructures.<sup>22</sup> Attempts to isolate individual macrocycles from the library for further characterization failed due to rapid re-equilibration.

Methanol as the co-solvent promotes the co-existence of two distinct polymorphs. Building block **1** (1.0 mM) first formed **1<sub>6</sub>** as the dominant species in the presence of 10% methanol in B<sub>2</sub>O<sub>3</sub> buffer. After 2 weeks, the library shifted to form more **1<sub>4</sub>** at the expense of **1<sub>6</sub>**, to yield a state in which the two macrocycles coexist (Fig. 4a). Cryo-TEM micrographs of the library at 2.5 months reveal both vesicles and fibres co-existing (Fig. 4d). Most vesicles were 50–100 nm in size, and exhibited a more spherical morphology and smooth surface (Fig. S11†) than the

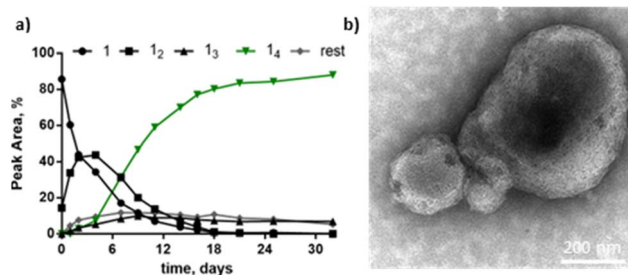


Fig. 2 (a) Larger quantities of 1-propanol (50%) promote the formation of **1<sub>4</sub>** and (b) yields vesicular structures as evident from TEM analysis (negative staining).

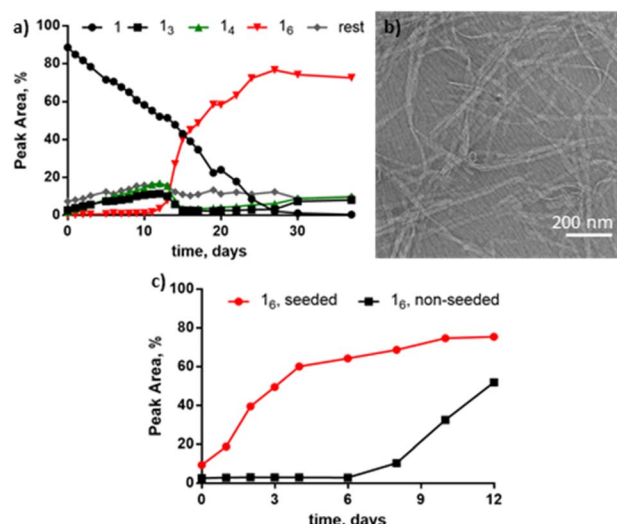


Fig. 3 (a) In the presence of 10% THF in B<sub>2</sub>O<sub>3</sub> buffer (50 mM, pH 8.0), **1<sub>6</sub>** emerges as the dominant species and (b) self-assembles into nanoribbons observed using TEM (negative staining). (c) Seeding experiments reveal that **1<sub>6</sub>** is a self-replicator as it grows faster in the presence of pre-formed **1<sub>6</sub>** seed (red) than without seed (black).





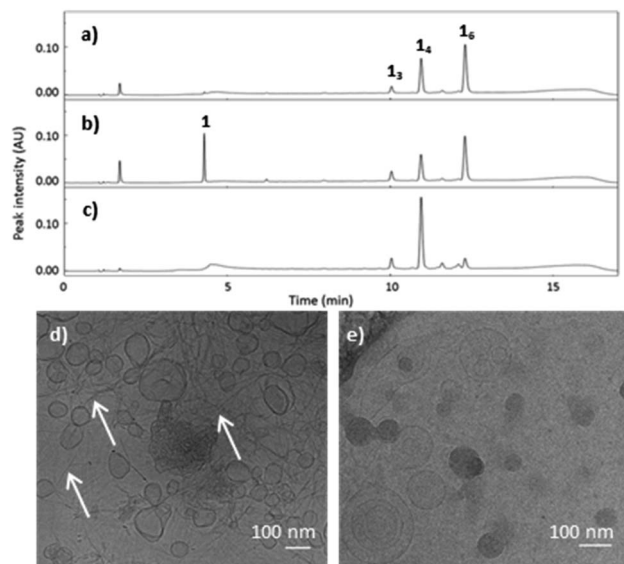


Fig. 4 UPLC chromatograms show that (a) slow oxidation of **1** in the presence of methanol (10%) yields both **1<sub>a</sub>** and **1<sub>b</sub>**. The corresponding cryo-TEM micrograph (d) shows the co-existence of fibres (highlighted by white arrows) and vesicles. (b) Reduction of the library by the addition of TCEP re-liberates **1** and (c) allows the system to re-equilibrate to form exclusively **1<sub>a</sub>**. (e) Cryo-TEM micrograph showing the presence of only vesicles after this treatment.

vesicular aggregates observed in the samples containing 50% 1-propanol, which featured surfaces with periodic patterns (Fig. S5†). After four months, **1<sub>b</sub>** was completely consumed and **1<sub>a</sub>** (along with smaller rings) became the dominant species. This suggests that **1<sub>b</sub>** produced a metastable phase while **1<sub>a</sub>** assembled into the thermodynamically more stable phase, in this particular solvent environment.

To confirm this difference in stability, the sample was partially reduced and allowed to re-oxidise, to promote thiol-mediated disulfide exchange. The addition of the reducing agent, tris(2-carboxyethyl)phosphine (TCEP) to the mixture containing **1<sub>b</sub>**, and **1<sub>a</sub>** (Fig. 4a) did not reveal any differences in stability or reactivity as all molecular species were reduced to approximately the same extent (Fig. 4b). The partially reduced library was left to exchange and oxidise, resulting in a shift in its composition towards **1<sub>a</sub>** after two weeks (Fig. 4c), in agreement with **1<sub>b</sub>** being a metastable species while **1<sub>a</sub>** prevails as the thermodynamic product. Cryo-TEM micrographs of the library containing **1<sub>a</sub>** show the presence of only vesicular structures and the absence of fibres (Fig. 4e). These observations suggest that the two molecular species (**1<sub>a</sub>** and **1<sub>b</sub>**) form two distinct supramolecular structures with **1<sub>a</sub>** as the main species present in vesicle membranes.

## Conclusions

By modulating the environment of DCLs made from a single building block through addition of various co-solvents, we were able to produce four different polymorphic structures: fibres, nanoribbons, and two different vesicle morphologies. Both fibres and nanoribbons were self-replicating supramolecular

structures, and in one set of conditions both fibres and vesicles transiently co-existed. Such significant differences in morphologies in a single building block system is important as each structure could in principle impart a unique functionality. For example, we have previously shown that self-replicating fibres derived from a DCL can catalyse catabolic reactions and bind to co-factors that enhance their formation.<sup>23</sup>

Furthermore, compartments are crucial components in the synthesis of life. They protect the system against parasitic molecules and provide an environment for colocalizing and concentrating substrates and allow for excretion of toxic by-products.

Previously, we have shown the emergence and co-existence of two different supramolecular structures (fibres and foldamers) from a two-building block DCL, while in another example another two-building block system yielded four unique supramolecular structures.<sup>24</sup> However, the ability to switch between significantly different polymorphs or creating both simultaneously, from a single-building-block DCL, as described herein, has not yet been reported.

The different polymorphs differ in the extent to which they can form through autocatalysis. The fibres and ribbons are formed autocatalytically, while the vesicles are not. We attribute this difference to the presence of catalytic sites at the ends of the fibres or ribbon. Previous work on peptide-based fibres has shown that the rate of replication is proportional to the fibre end concentration, where precursors were found to accumulate.<sup>25</sup> Such catalytic sites are likely to be absent in the vesicles, as these are closed structures.

The fact that replication and vesicle-type compartments can form from the same building block and even transiently co-exist is intriguing from the perspective of the emergence of life, which requires replication and compartmentalisation.

From the observation that the switchover from one assembly morphology to another is accompanied by a change in covalent bonds (*i.e.*, a change in the ring size of the macrocycles that assemble) we conclude that the mutual interplay between covalent bond formation and noncovalent interactions promotes polymorphism, and, through that, adaptability. Although the types of building blocks and conditions used in this study are not all prebiotically plausible, this work demonstrates the concept of structural adaption of synthetic systems in a response to a change in environment; one of many conditions needed for evolution. Thus, systems that allow for covalent and non-covalent dynamics appear particularly promising in the context of achieving evolutionary adaptations.

## Data availability

The raw data generated and analysed during the current study are available from the authors on reasonable request.

## Author contributions

BB designed and carried out most of the experiments and wrote the first draft of the manuscript. AK and MAB placed the work in the broader context of polymorphism and co-wrote the



manuscript. MA and GMS performed analytic experiments. SO supervised the project and co-wrote the article.

## Conflicts of interest

There are no conflicts to declare.

## Acknowledgements

This research was supported by the ERC (AdG 741774), the NWO (VICI grant 724.012.002), Marie Skłodowska-Curie Grants (642192 and 101028779) and the Dutch Ministry of Education, Culture and Science (Gravitation Program 024.001.035).

## Notes and references

- 1 I. Budin and J. W. Szostak, *Annu. Rev. Biophys.*, 2010, **39**, 245–263.
- 2 C. K. Ghilambor, J. K. McKay, S. P. Carroll and D. N. Reznick, *Funct. Ecol.*, 2007, **21**, 394–407.
- 3 P. M. Sheppard, *J. Med. Genet.*, 1971, **8**, 545–546.
- 4 J. Adamcik and R. Mezzenga, *Angew. Chem., Int. Ed.*, 2018, **57**, 8370–8382.
- 5 C. Gao and G. Chen, *Acc. Chem. Res.*, 2020, **53**, 740–751.
- 6 B. d. Kruijff, *Curr. Opin. Chem. Biol.*, 1997, **1**, 564–569.
- 7 K. Ohtsubo and J. D. Marth, *Cell*, 2006, **126**, 855–867.
- 8 K. Namba and G. Stubbs, *Science*, 1986, **231**, 1401–1406.
- 9 F. Tantakitti, J. Boekhoven, X. Wang, R. V. Kazantsev, T. Yu, J. Li, E. Zhuang, R. Zandi, J. H. Ortony, C. J. Newcomb, L. C. Palmer, G. S. Shekhawat, M. O. de la Cruz, G. C. Schatz and S. I. Stupp, *Nat. Mater.*, 2016, **15**, 469–476.
- 10 (a) B. Moulton and M. J. Zaworotko, *Chem. Rev.*, 2001, **101**, 1629–1658; (b) A. Langenstroer, K. K. Kartha, Y. Dorca, J. Droste, V. Stepanenko, R. Q. Albuquerque, M. R. Hansen, L. Sánchez and G. Fernández, *J. Am. Chem. Soc.*, 2019, **141**, 5192–5200; (c) Y. La, T. H. An, T. J. Shin, C. Park and K. T. Kim, *Angew. Chem., Int. Ed.*, 2015, **54**, 10483–10487; (d) D. Mandal, S. Dinda, P. Choudhury and P. K. Das, *Langmuir*, 2016, **32**, 9780–9789; (e) Y. Gao, J. Hao, J. Wu, X. Zhang, J. Hu and Y. Ju, *Langmuir*, 2016, **32**, 1685–1692; (f) P. A. Korevaar, S. J. George, A. J. Markvoort, M. M. J. Smulders, P. A. J. Hilbers, A. P. H. J. Schenning, T. F. A. De Greef and E. W. Meijer, *Nature*, 2012, **481**, 492–496; (g) B. Kemper, L. Zengerling, D. Spitzer, R. Otter, T. Bauer and P. Besenius, *J. Am. Chem. Soc.*, 2018, **140**, 534–537; (h) A. Aliprandi, M. Mauro and L. De Cola, *Nat. Chem.*, 2016, **8**, 10–15.
- 11 N. M. Matsumoto, R. P. M. Lafleur, X. Lou, K.-C. Shih, S. P. W. Wijnands, C. Guibert, J. W. A. M. van Rosendaal, I. K. Voets, A. R. A. Palmans, Y. Lin and E. W. Meijer, *J. Am. Chem. Soc.*, 2018, **140**, 13308–13316.
- 12 N. J. Van Zee, B. Adelizzi, M. F. J. Mabesoone, X. Meng, A. Aloï, R. H. Zha, M. Lutz, I. A. W. Pilot, A. R. A. Palmans and E. W. Meijer, *Nature*, 2018, **558**, 100–103.
- 13 (a) F. B. L. Cougnon and J. K. M. Sanders, *Acc. Chem. Res.*, 2012, **45**, 2211–2221; (b) E. Moulin, G. Cormos and N. Giuseppone, *Chem. Soc. Rev.*, 2012, **41**, 1031–1049; (c) S. Ladame, *Org. Biomol. Chem.*, 2008, **6**, 219–226; (d) P. T. Corbett, J. Leclaire, L. Vial, K. R. West, J.-L. Wietor, J. K. M. Sanders and S. Otto, *Chem. Rev.*, 2006, **106**, 3652–3711.
- 14 J. M. A. Carnall, C. A. Waudby, A. M. Belenguer, M. C. A. Stuart, J. J.-P. Peyralans and S. Otto, *Science*, 2010, **327**, 1502–1506.
- 15 B. Bartolec, G. Leonetti, J. Li, W. Smit, M. Altay, G. Monreal Santiago, Y. Yan and S. Otto, *Langmuir*, 2019, **35**, 5787–5792.
- 16 D. E. Discher and A. Eisenberg, *Science*, 2002, **297**, 967–973.
- 17 (a) J. Boekhoven, A. M. Brizard, P. van Rijn, M. C. A. Stuart, R. Eelkema and J. H. van Esch, *Angew. Chem., Int. Ed.*, 2011, **50**, 12285–12289; (b) R. P. M. Lafleur, X. Lou, G. M. Pavan, A. R. A. Palmans and E. W. Meijer, *Chem. Sci.*, 2018, **9**, 6199–6209.
- 18 G. Schaeffer, M. J. Eleveld, J. Ottel  , P. C. Kroon, P. W. J. M. Frederix, S. Yang and S. Otto, *J. Am. Chem. Soc.*, 2022, **144**, 6291–6297.
- 19 M. Malakoutikhah, J. J. P. Peyralans, M. Colomb-Delsuc, H. Fanlo-Virgos, M. C. A. Stuart and S. Otto, *J. Am. Chem. Soc.*, 2013, **135**, 18406–18417.
- 20 A. D. Bangham, M. M. Standish and J. C. Watkins, *J. Mol. Biol.*, 1965, **13**, 238–252.
- 21 J. N. Israelachvili, H. E. Mitchel and J. Ninham, *J. Chem. Soc., Faraday Trans. 2*, 1976, **72**, 1525.
- 22 B. Rubinov, N. Wagner, M. Matmor, O. Regev, N. Ashkenasy and G. Ashkenasy, *ACS Nano*, 2012, **6**, 7893–7901.
- 23 (a) J. Ottel  , A. S. Hussain, C. Mayer and S. Otto, *Nat. Catal.*, 2020, **3**, 547–553; (b) G. Monreal Santiago, K. Liu, W. R. Browne and S. Otto, *Nat. Chem.*, 2020, **12**, 603–607.
- 24 (a) B. Liu, M. A. Beatty, C. G. Pappas, K. Liu, J. Ottel   and S. Otto, *Angew. Chem., Int. Ed.*, 2021, **60**, 13569–13573; (b) D. Kom  romy, T. Tiemersma-Wegman, J. Kemmink, G. Portale, P. R. Adamski, A. Blokhuis, F. S. Aalbers, I. Mari  , G. M. Santiago, J. Ottel  , A. Sood, V. Saggiomo, B. Liu, P. van der Meulen and S. Otto, *Chem*, 2021, **7**, 1933–1951.
- 25 (a) M. Colomb-Delsuc, E. Mattia, J. W. Sadownik and S. Otto, *Nat. Commun.*, 2015, **6**, 7427; (b) S. Maity, J. Ottele, G. M. Santiago, P. Frederix, P. Kroon, O. Markovitch, M. C. A. Stuart, S. J. Marrink, S. Otto and W. H. Roos, *J. Am. Chem. Soc.*, 2020, **142**, 13709–13717.

